

First Annual Musculoskeletal Collaboration Center Research Day

September 16, 2023

Engineering Research Building, Virginia Commonwealth University

Thank you for joining the Musculoskeletal Collaboration Center (MC2) for its first annual Research Day. We are a research-intensive working group between the Departments of Orthopaedic Surgery and Biomedical Engineering at Virginia Commonwealth University (VCU). Our group is dedicated to advancing musculoskeletal knowledge through innovative research, education, and clinical practice. Please direct all inquiries to Jonathan Boyd at jonathan.boyd@vcuhealth.org.

AGENDA

Time	Event	Presenter	Location
7:15	Poster setup and light breakfast graciously donated by the Institute for Engineering and Medicine		Collaboration Hub
8:00	Welcome and Introductory Remarks	Jonathan Boyd, Ph.D.	ERB1313
8:10	“Healing trajectory of fractured bone and muscle tissues in spaceflight”	Nabarun Chakraborty, Ph.D., WRAIR	ERB1313 (Zoom)
8:30	“Science in Space: Does Space Travel Accelerate Aging?”	Henry Donahue, Ph.D.	ERB1313
8:45	“Contribution of Immune Cells to Bone Healing and Regeneration”	Rene Olivares-Navarette, DDS, Ph.D.	ERB1313
9:00	“Usability of Nerve Tape: A Novel Sutureless Nerve Coaptation Device”	Jonathan Isaacs, M.D.	ERB1313
9:15	BREAK		
9:30	“Driving Collagen Fiber Formation for Functional Musculoskeletal Repair and Replacement”	Jennifer Puetzer, Ph.D.	ERB1313
9:45	“Nerve Tape is an effective tool for small nerve repair”	Geetanjali Bendale, Ph.D.	ERB1313
10:00	“Advancements in Upper Limb Rehabilitation after Spinal Cord Injury”	Carrie Peterson, Ph.D.	ERB1313
10:15	“Transitioning Fields from PhD to Postdoc: Leveraging an Orthopaedic Research Background into New Research Areas”	Nicole Prince, Ph.D., Harvard Medical School	ERB1313 (Zoom)
10:30	Poster Session Begins		Collaboration Hub
11:45	Poster Awards	Jonathan Boyd, Ph.D.	ERB1313

POSTER PRESENTATIONS

POSTER 1: Impact of Age of Spinal Cord Injury Onset on Peak Rotator Cuff Forces during Manual Wheelchair Propulsion. Zhao H., Cho, Y., Schnorenberg, A.J., Slavens, B.A., Peterson, C.L.

POSTER 2: DMP1 Lineage Connexin43 Deficiency Attenuates Decreases in Skeletal Muscle Strength and Fracture Callus Mineralization During Hindlimb Unloading. Evan G. Buettmann, Gabriel A. Hoppock, Lovell B. Abraham, Rachel C. DeNapoli, Jessica R. Cornthwaite, Joseph A. Denisco, Jerin Jose, Michael A. Friedman, Yue Zhang, Jolene J. Windle, Michael J. McClure, Henry J. Donahue

POSTER 3: Osteoblast-derived Matrix Vesicle small RNAs May Contribute to Retention of an Osteoprogenitor Cell Phenotype in Mature Bone. Anne Skelton, David J. Cohen, Zvi Schwartz, Barbara D. Boyan

POSTER 4: Developmental-like Slow Stretch Drives Hierarchical Fiber Formation in a Dose-and Organization-Dependent Way. Kelly R. Ott, Jennifer L. Puetzer

POSTER 5: ELISpot Quantification of anti-Isd and anti-Atl Plasma Cells. John Owen, Stephen Kates, Gowrishankar Muthukrishnan, David Topham, Edward Schwarz

POSTER 6: Reduction of Neutrophil Extracellular Traps Accelerates Inflammatory Resolution and Increases Bone Formation on Titanium Implants. Lais Morandini, Derek Avery, Benjamin Angeles, Paul Winston, Rebecca K. Martin, Henry J. Donahue, Rene Olivares-Navarrete

POSTER 7: Scaling a Generic Upper Limb Musculoskeletal Model to Represent Individuals with Paraplegia. Cho Y., Zhao H., Schnorenberg, A.J., Slavens, B.A., Peterson, C.L.

POSTER 8: Induced Pseudomembrane Enrichment in Long Nerve Allograft Reconstruction. Omar Protzuk, Mariam Samuel, Kristin Seward, Chris Keshishian, Geetanjali Bendale, Jonathan Isaacs

POSTER 9: Osteocyte-specific endocannabinoid receptor 1 (CB1) deficiency influences cancellous bone mass, but does not affect bone response to disuse. Rachel C. DeNapoli, Evan G. Buettmann, Jolene J. Windle, Aron H. Lichtman, Henry J. Donahue

POSTER 10: Effect of Cyclic Stretch in Engineered Ligaments Depends on Degree of Hierarchical Collagen Organization. Leia Troop and Jennifer L. Puetzer

POSTER 11: T cells Contribute to Macrophage Polarization and MSC Recruitment During Osseointegration. Derek Avery, Lais Morandini, Melissa Gabrieic, Luke Sheakley, Matthieu Peralta, Henry J. Donahue, Rebecca K. Martin, Rene Olivares-Navarrete

POSTER 12: Non-alcoholic fatty liver disease is associated with skeletal fragility in DIAMOND mice. Galen M Goldscheitter, Alexandra M Hooks, Mulugeta Seneshaw, Evan G Buettmann, Arun J Sanyal, Henry J Donahue

POSTER 13: Estrogen induced osteolysis in triple negative breast cancer mediated by estrogen receptor alpha 36. David J Cohen, Cydney Dennis, Jingyao Deng, Zvi Schwartz, Barbara D Boyan

POSTER 14: The Effect of Genetic Variability on Muscle Mass and Strength from Disuse. Jessica R. Cornthwaite, Michael A. Friedman, Henry J. Donahue

POSTER 15: Investigating the Role of Focal Adhesion Kinase in Hierarchical Collagen Fiber Formation for Musculoskeletal Repair. Tristan Strayer, Leia Troop, and Jennifer L. Puetzer

POSTER 16: Axial Compression of Tibia Increases Marrow Macrophage and T-Cell Subsets in a Load-Dependent Manner. Evan G. Buettmann, Lais Morandini, Joseph A. Denisco, Jerin Jose, Galen Goldscheitter, Michael A. Friedman, Henry J. Donahue, Rene Olivares-Navarrete

POSTER 17: Unraveling the Role of Advanced Glycation End-Products in Age-Related Human Meniscus Degeneration. Austin G. Gouldin, Nirav K. Patel, Gregory J. Golladay, Jennifer L. Puetzer

POSTER 18: Genetic Variation Affects the Magnitude of Bone and Muscle Loss from Disuse. Michael A. Friedman, Jessica Cornthwaite, John McKean, Zhane Davis, Gabriel A. Hoppock, Yue Zhang, Evan G. Buettmann, Steven Meas, Gabriella M. Daire, Charles R. Farber, Henry J. Donahue

POSTER 19: Hindlimb Unloading Induces Microarchitectural and Transcriptomic Changes in the Femur and Tibia in an Age- and Sex-Dependent Manner. Steven J. Meas, Michael A. Friedman, Gabriella M. Daire, Henry J Donahue

POSTER 20: Characterizing Nucleus Pulposus fluid shear stresses and deformation in response to interstitial fluid flow in healthy and degenerate microenvironments. Logan Petry, Joyce Xu, Priscilla Y Hwang

POSTER 21: Bolus Fentanyl Induces Prolonged Cardiovascular Dysregulation in SKH-1 Mice. Mackenzie Newman, Heather Connery, John Owen, Raymond Raylman, Jonathan Boyd

POSTER 22: RNA Sequencing Analysis of Muscle-Nerve Cross-talk in a Transwell Co-culture Model. James T Redden, Zvi Schwartz, Michael J. McClure

1. Impact of Age of Spinal Cord Injury Onset on Peak Rotator Cuff Forces during Manual Wheelchair Propulsion

Zhao H.¹, Cho, Y.¹, Schnorenberg, A.J.², Slavens, B.A.², Peterson, C.L.¹

¹Virginia Commonwealth University, ²University of Wisconsin-Milwaukee

Manual wheelchair usage is widespread (over 3 million users in the US) and serves as the primary method of mobility for many individuals with paraplegia after spinal cord injury (SCI) [1]. Manual wheelchair users with paraplegia have reported high incidence of shoulder pain along with nearly all manual wheelchair users exhibiting some form of shoulder pathology [2]. Surprisingly, adults with pediatric-onset of SCI were found to have lower incidence of shoulder pain relative to adults with adult-onset of SCI despite having more years of wheelchair use [2]. Large rotator cuff muscle forces and glenohumeral joint contact forces presumably increase the risk for shoulder pain. As such, we expect that peak rotator cuff muscle forces and glenohumeral joint contact forces will be greater in those with adult-onset SCI relative to pediatric-onset SCI. The goal of our work is to determine the impact of age of SCI onset on peak rotator cuff muscle forces and glenohumeral joint contact forces during wheelchair propulsion. Kinematic and kinetic data were recorded as 40 participants propelled an instrumented wheelchair at their self-selected speed. Data from select participants were processed through OpenSim utilities using a scapulothoracic shoulder model [3] that was adapted to include forearm and wrist muscles from Saul et al. [4]. Predicted peak rotator cuff forces and joint contact forces were higher relative to other studies investigating patients with paraplegia [5]. However, our study utilizes a more robust shoulder model along with additional muscles [3][4]. Preliminary results suggest differences in shoulder muscle and joint forces during wheelchair propulsion among three subjects from our groups of interest: children, adults with pediatric-onset of SCI, and adults with adult-onset of SCI. Further analysis will lead to characterization of potential differences and help identify key factors that result in shoulder pain and pathology.

References: [1] Schnorenberg, A. J., et al., *J. Biomech.* 2014 47(1), 269–276. [2] Brose, S. W., et al., *Arch Phys Med Rehabil* 2008 89(11), 2086–2093. [3] Seth, A., et al., *PLOS ONE* 2016 11(1), e0141028. [4] Saul K, et al. *Comput Methods Biomech Biomed Engin.* 2015;18(13):1445–1458. [5] van Drongelen, S., et al., *Arch Phys Med Rehabil* 2005. 86(7), 1434–1440.

2. DMP1 Lineage Connexin43 Deficiency Attenuates Decreases in Skeletal Muscle Strength and Fracture Callus Mineralization During Hindlimb Unloading

Evan G. Buettmann¹, Gabriel A. Hoppock¹, Lovell B. Abraham¹, Rachel C. DeNapoli¹, Jessica R. Cornthwaite¹, Joseph A. Denisco¹, Jerin Jose¹, Michael A. Friedman¹, Yue Zhang¹, Jolene J. Windle², Michael J. McClure¹, Henry J. Donahue¹

¹Department of Biomedical Engineering, ²Department of Human and Molecular Genetics, Virginia Commonwealth University, Richmond, VA

Introduction: Preclinical studies suggests that deletion of the predominate gap junction protein connexin 43 (Cx43), decreases bone and muscle strength and impairs fracture healing under conditions of normal weight-bearing ambulation.¹⁻³ Emerging data from our lab suggests that Cx43 deficiency during hindlimb unloading (HLU) attenuates bone loss.^{4,5} However, the role that Cx43 deficiency plays in fracture healing and muscle strength during HLU remains unknown.

Methods: Cx43 cKO animals consisted of female C57BL/6J (26 weeks) mice harboring DMP1 Cre and GJA1^{fl/fl} alleles⁶. Littermate Cre negative mice (WT) served as controls. All mice underwent HLU or normal weight-bearing activity (controls) for 3 weeks. Then mice had their right femur fractured and were allowed to heal for 14 days (DPF14). Data was analyzed for effect of treatment (HLU, control) and genotype (WT, Cx43 cKO) by 2-WAY repeated measures ANOVA with Tukey's multiple comparisons test (*p< 0.05).

Results: WT mice showed significant loss of normalized gastrocnemius mass, tetanic force output and callus mineralization due to HLU. In contrast, Cx43 cKO mice were protected from changes in tetanic force output and callus mineralization due to HLU compared to littermate controls (p<0.05; **Figure 1**). In uninjured diaphyseal femurs, HLU and Cx43 deficiency synergistically decreased cortical and metaphyseal bone volume (p<0.05; ~2-3 fold relative to controls).

Discussion: Our results suggest that Cx43 deficiency in DMP1 lineage cells may protect against impairments in muscle function with HLU and later callus mechanosensation with unloading. These muscle results contrast with those seen previously in Cx43 deficient male aged mice⁷. Future work will use the inducible DMP1 Cre_ERT2⁸, which demonstrates reduced muscle targeting compared to DMP1 Cre mice, to see if postnatal Cx43 deletion in bone alters this phenotype.

Acknowledgements: This work is supported by the Translational Research Institute through NASA Cooperative Agreement NNX16AO69A

References:

1. Shen, H., et al., *Deletion of connexin43 in osteoblasts/osteocytes leads to impaired muscle formation in mice*. J Bone Miner Res, 2015. **30**(4): p. 596-605.
2. Loiselle, A.E., et al., *Osteoblast and osteocyte-specific loss of Connexin43 results in delayed bone formation and healing during murine fracture healing*. J Orthop Res, 2013. **31**(1): p. 147-54.
3. Bivi, N., et al., *Cell autonomous requirement of connexin 43 for osteocyte survival: consequences for endocortical resorption and periosteal bone formation*. J Bone Miner Res, 2012. **27**(2): p. 374-89.
4. Lloyd, S.A., et al., *Connexin 43 deficiency attenuates loss of trabecular bone and prevents suppression of cortical bone formation during unloading*. J Bone Miner Res, 2012. **27**(11): p. 2359-72.
5. Grimston, S.K., et al., *Connexin43 deficiency reduces the sensitivity of cortical bone to the effects of muscle paralysis*. J Bone Miner Res, 2011. **26**(9): p. 2151-60.
6. Lu, Y., et al., *DMP1-targeted Cre expression in odontoblasts and osteocytes*. J Dent Res, 2007. **86**(4): p. 320-5.
7. Li, G., et al., *Osteocytic Connexin43 Channels Regulate Bone-Muscle Crosstalk*. Cells, 2021. **10**(2).
8. Kim, S.W., et al., *Intermittent parathyroid hormone administration converts quiescent lining cells to active osteoblasts*. J Bone Miner Res, 2012. **27**(10): p. 2075-84.

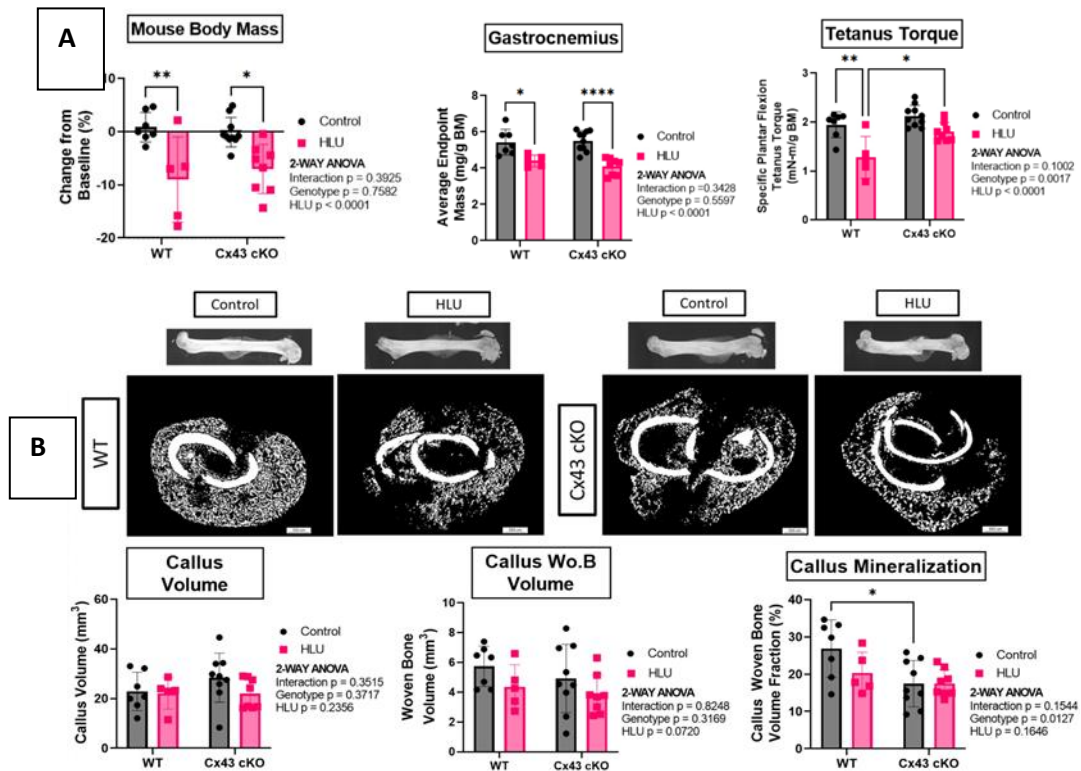


Figure 1. A. Changes in murine body mass, hindlimb skeletal muscle mass and max plantar flexion torque at DPF14. Masses were recorded by analytical balance. Triceps surae tetany was measured by Aurora 1300 and normalized by mouse body mass. **** p < 0.00005 * p < 0.05 by Tukey's post-hoc test following 2-WAY ANOVA; data presented as mean ± SD **B:** Callus woven bone formation and callus bone volume fracture (excluding original cortical bone) was computed for 600 slices centered around the fracture midpoint of each bone. **** p < 0.00005 * p < 0.05 by Tukey's post-hoc test following 2-WAY ANOVA; data presented as mean ± SD

3. Osteoblast-derived Matrix Vesicle small RNAs May Contribute to Retention of an Osteoprogenitor Cell Phenotype in Mature Bone (150 Characters with spaces; currently 125)

Anne Skelton¹, David J. Cohen², Zvi Schwartz^{2,3}, Barbara D. Boyan^{2,4}.

¹Dept. of Physiology and Biophysics and ²Dept. of Biomedical Engineering, Virginia Commonwealth University, Richmond, Virginia, USA. ³Dept. of Periodontics, University of Texas Health Science Center at San Antonio, San Antonio, Texas, USA. ⁴Wallace H. Coulter Dept. of Biomedical Engineering, Georgia Institute of Technology, Atlanta, Georgia, USA.

INTRODUCTION: Matrix vesicles (MVs) are nano-sized extracellular vesicles that are released by mineralization-competent cells and become anchored in the extracellular matrix (ECM). They have historically been involved in mineral formation during endochondral ossification, but further research has revealed they contain proteins and microRNA that point to roles in cell regulation and inter-cellular communication. **PURPOSE:** This study performed an in-depth analysis of the microRNA cargo within osteoblast-derived matrix vesicles and established the role of these vesicles using cells at two different levels of osteoblastic differentiation. **METHODS:** MVs were isolated from the trypsin digested ECM of MG-63 and MC3T3-E1 osteoblast-like cells. MVs and respective cell lysates underwent small RNA sequencing with differential expression analysis to evaluate the unique MV microRNA cargo. MVs were also isolated from confluent cultures of MG-63 cells grown in growth medium and MG-63 cells grown in osteogenic differentiation medium for 10 days. MG-63 cells in growth medium were treated with these MVs for 24 and 48 hours followed by harvest and assessment of osteoblastic differentiation and production of inflammatory markers. **RESULTS:** Small RNA differential expression confirmed distinct enrichment of microRNA within the MVs with 52 upregulated microRNAs in MG-63-derived vesicles and 51 upregulated microRNAs in MC3T3-E1-derived vesicles. Pathway analysis of upregulated microRNA suggested preferential targeting of transcription pathways, particularly those regulated by RUNX3 and MECP. Additionally, several upregulated microRNA were found to be anti-osteogenic when searched in the literature. Following treatment of confluent cultures with MVs for 24 and 48 hours, alkaline phosphatase specific activity was decreased and production of osteocalcin, vascular endothelial growth factor (VEGF), and interleukin-6 (IL-6) were decreased, but there were no changes in DNA content. Similar results were observed when cells were treated for 24 and 48 hours with MVs harvested after 10 days of growth in osteogenic medium. **CONCLUSIONS:** Small RNA sequencing suggests that microRNAs are selectively packaged into MVs by their parent cells with targeting of transcription factors that may be responsible for their role in osteogenesis. The information found in the literature regarding upregulated microRNAs correlates with our in vitro data, indicating that MVs may contribute to bone formation and remodeling in a more nuanced manner, particularly in relation to osteoblasts, other cells found within mature bone, and other types of extracellular vesicles released by these cells.

4. Developmental-like Slow Stretch Drives Hierarchical Fiber Formation in a Dose- and Organization-Dependent Way

Kelly R. Ott¹, Jennifer L. Puetzer^{1,2}

Departments of ¹Biomedical Engineering and ²Orthopaedic Surgery, Virginia Commonwealth University

Objective: Hierarchical collagen fibers are the main source of strength in tendons and ligaments. These fibers do not regenerate post-injury, limiting treatment options. Previously, our lab developed a static culture system that guides ACL fibroblasts to develop hierarchical collagen fibers over 6 weeks, but further maturation is needed to be functional replacements. Mechanical cues, such as steady growth, are necessary for *in vivo* maturation, but growth-rates vary more than 10-fold during early stages of ACL development, while there are significant changes in collagen organization. The objective of this study was to investigate whether slow elongation at rates similar to neonatal and postnatal ACL growth-rates differentially drive hierarchical fiber formation and whether the effect of these loads vary at different levels of organization.

Methods: ACL fibroblasts were seeded into 20 mg/mL collagen gels at 5×10^6 cells/mL to form constructs. To evaluate the effect of stretch applied to collagen at the unorganized, fibril, or fiber level, constructs were cultured in our static device for 0, 2, or 4 weeks, respectively, and then stretched at postnatal (0.1 mm/day) or neonatal (1 mm/day) growth-rates for 1 to 3 weeks using a tensile bioreactor. Post-culture, collagen organization, matrix composition, and tensile mechanical properties were evaluated.

Results: Prolonged stretch increased collagen organization, composition, and tissue mechanics in a dose-dependent manner. Stretch increased collagen organization at all levels of organization, but changes in composition and tissue mechanics depended on the timing and rate of stretch, with neonatal-rates having the largest effect in unorganized gels and postnatal-rates having the largest effect at the fibril or fiber level. Collectively, this demonstrates cells sense and respond to stretch differentially depending on the degree of organization.

Conclusion: This study provides new insight into how growth-rates regulate cellular fiber formation, which will help engineered replacements and inform rehabilitation protocols to drive repair.

5. ELISpot Quantification of anti-Isd and anti-Atl Plasma Cells

Owen JR¹, Kates SL¹, Muthukrishnan G², Topham DJ², Schwarz EM²

¹Department of Orthopaedic Surgery, Virginia Commonwealth University, Richmond, Virginia, USA.

²Center for Musculoskeletal Research, University of Rochester Medical Center, Rochester, New York, USA.

Staphylococcus aureus induced osteomyelitis remains a challenge for orthopaedic surgery. Anti-glucosaminidase (anti-Gmd) antibodies, an anti-autolysin (anti-Atl), are protective against *S. aureus* infections while anti-Iron surface determinant B (anti-IsdB) antibodies are susceptible determinants.^{1,2} Furthermore, most people have a susceptible anti-*S. aureus* immune proteome (low anti-Gmd/high anti-IsdB). We hypothesize that this native susceptible immune proteome is caused by a defect in anti-Gmd vs. anti-IsdB antibody secreting B cells, plasmablasts and/or long-lived plasma cells (LLPCs). We will investigate the mechanism(s) of the susceptible anti-*S. aureus* immune proteome by quantifying anti-Gmd vs. anti-IsdB specific B cells and plasmablasts in blood, and LLPCs in bone marrow and correlate this with circulating antibody levels through a clinical pilot study of patients having elective Total Hip Replacements (THR) or THR revision surgery for *S. aureus* infection, versus healthy controls. We must first develop enzyme-linked immunosorbent spot (ELISpot) assays for *S. aureus* specific antibody secreting cells from blood and bone marrow. In a pilot study of uninfected patients, we are adapting ELISpot protocols already developed for other antigens.³ We show initial success from our most recent ELISpot assay of blood and bone marrow memory B-cells. Uninfected blood and bone marrow samples from other subjects will allow optimization of the protocols and to establish expectations for reproducibility and variation between subjects. Once protocols are finalized, the clinical study of THR or THR revision surgery for *S. aureus* infection will be conducted as a critical step toward discovering the mechanism(s) behind the genesis of the susceptible anti-*S. aureus* immune proteome.

References:

1. Lee CC, Southgate RD, Jiao C, Gersz E, Owen JR, Kates SL, Beck CA, Xie C, Daiss JL, Post V, Moriarty TF, Zeiter S, Schwarz EM, Muthukrishnan G. Deriving a dose and regimen for anti-glucosaminidase antibody passive-immunisation for patients with *Staphylococcus aureus* osteomyelitis. *Eur Cell Mater*. 2020 Jan 31;39:96-107. doi: 10.22203/eCM.v039a06.
2. Kates SL, Owen JR, Beck CA, Xie C, Muthukrishnan G, Daiss JL, Schwarz EM. Lack of Humoral Immunity Against Glucosaminidase Is Associated with Postoperative Complications in *Staphylococcus aureus* Osteomyelitis. *J Bone Joint Surg Am*. 2020 Nov 4;102(21):1842-1848. doi: 10.2106/JBJS.20.00029.
3. Nguyen-Contant P, Embong AK, Topham DJ, Sangster MY. Analysis of Antigen-Specific Human Memory B Cell Populations Based on In Vitro Polyclonal Stimulation. *Curr Protoc Immunol*. 2020 Dec;131(1):e109. doi: 10.1002/cpim.109.

6. Reduction of Neutrophil Extracellular Traps Accelerates Inflammatory Resolution and Increases Bone Formation on Titanium Implants

Lais Morandini¹, Derek Avery¹, Benjamin Angeles¹, Paul Winston¹, Rebecca K. Martin², Henry J. Donahue¹, Rene Olivares-Navarrete¹

¹Department of Biomedical Engineering, College of Engineering, Virginia Commonwealth University, Richmond, VA

²Department of Microbiology and Immunology, School of Medicine, Virginia Commonwealth University, Richmond, VA

Objective: Neutrophils are the first cells to be recruited at the site of biomaterial implantation and release DNA-based networks called neutrophil extracellular traps (NETs) that can affect healing. The aim of this work was to evaluate the effect of NETs on inflammatory events and osteointegration after biomaterial implantation.

Methodology: Smooth, rough, or rough-hydrophilic titanium implants were placed in the femur of C57BL/6J control mice or transgenic mice null for myeloperoxidase (*Mpo*^{-/-}), elastase (*Elane*^{-/-}), or peptidyl arginine deiminase 4 (*Padi4*^{-/-}). Animals (n=6) were harvested 12 hours, 1 day, 3 days, 5 days, or 7 days following biomaterial implantation for flow cytometry and ELISA analysis or 21 days for Micro CT. Neutrophils were isolated from these mouse strains and plated on smooth, rough, or rough-hydrophilic Ti surfaces. After 4 hours, conditioned media was collected for ELISA quantification. Macrophages and Neutrophils co-culture was performed, and conditioned media was collected for ELISA. Cells were detached and collected for flow cytometry analysis.

Results: Recruitment of neutrophils and pro-inflammatory macrophages were reduced at all time points analyzed for all Ti implants in *Padi4* mice. PAD4 or peptidyl arginine deiminase-4, catalyzes arginine residues to citrulline in histones resulting in chromatin decondensation and subsequent NET formation. Ablation of *Padi4* resulted in the highest levels of anti-inflammatory macrophages in all Ti implants. *Padi4* significantly reduced NET formation at all time points and implants. Neutrophils from *Padi4* and *MPO* showed the highest production of anti-inflammatory cytokines and caused anti-inflammatory macrophage activation on all Ti surfaces. Rough-hydrophilic surfaces induced the lowest NE, MPO, and NET formation. MSC recruitment and implant/bone contact were increased in *Padi4* mice in all implant types tested.

Conclusion: Our findings show the importance of neutrophils and NETs in the healing of implanted biomaterials and their influence on immune cells and osteointegration.

7. Scaling a Generic Upper Limb Musculoskeletal Model to Represent Individuals with Paraplegia

Cho Y.¹, Zhao H.¹, Schnorenberg, A.J.², Slavens, B.A.², Peterson, C.L.¹
¹ Virginia Commonwealth University, ² University of Wisconsin-Milwaukee

Musculoskeletal modeling and simulation of human movement is utilized for many biomechanical analyses. For analyses that require accurate representation of an individual's strength and limb lengths, a generic upper limb model can be scaled when developing subject-specific models is not feasible. A generic model can be anthropometrically scaled to represent a nonimpaired adult or child using regression equations. This approach previously showed that predicted maximum isometric shoulder moments correlated to moments measured experimentally from the same nonimpaired individuals. The objective of this study was to determine whether this scaling approach accurately represents the strength of adults and children with paraplegia.

Forty participants with paraplegia performed maximum isometric voluntary contractions while seated in a dynamometer to measure maximum moments of the shoulder and elbow joint. A generic model was scaled using linear regressions to predict total muscle volume and limb length from the individual's total height and body weight, respectively. The predicted total shoulder muscle volume was portioned into the upper limb muscle groups following the proportions of the generic model. Peak isometric muscle force was calculated from individual muscle volumes, muscle specific tension, and optimal fiber lengths from length-scaled models. Assuming full excitation of agonist muscles, the scaled models were used to compute predicted maximum moments in the same arm postures as the experiments. Mean absolute error (MAE) was calculated between the predicted and measured moments for each participant and arm position.

The moments with the largest MAE were shoulder extension and shoulder internal rotation (0.751 and 0.765). The moment with the smallest MAE was shoulder abduction (0.137). The high error between model predicted and measured elbow and shoulder moments suggests more direct measures of individual muscle strength and muscle size are needed to represent individuals with paraplegia.

8. Induced Pseudomembrane Enrichment in Long Nerve Allograft Reconstruction.

Omar Protzuk, MD, Mariam Samuel, Kristin Seward, Chris Keshishian, Geetanjali Bendale PhD, Jonathan Isaacs, MD

Introduction

Long nerve defects are typically reconstructed with autograft or processed acellular nerve allograft (PNA). PNA is convenient and avoids donor morbidity, but lacks the intense neurotrophic environment found in autograft, limiting their effective length. Extrapolating from the observation that pseudo-membranes induced around artificial implants have a rich trophic microenvironment, we recently demonstrated increased levels of neurotrophic factors in biological membranes induced around silicone rods implanted between rodent nerve ends. We hypothesize that nerve regeneration across PNA would be enhanced when inset within the induced pseudo-membrane tunnel.

Methods

Lewis rats (n=24) underwent resection of a 15mm sciatic nerve segment. The defect was filled with a silicone tube or nerve ends were secured to muscle bed. After 4 weeks, for the experimental group, the silicone rod was replaced with appropriately sized PNA threaded within the pseudo-membrane tunnel while the control groups received only PNA. Weekly ambulation videos were collected to assess sciatic function index (SFI). Twelve weeks post repair, outcome measures included muscle mass and girth, twitch and tetanic muscle contraction force, and nerve histomorphology.

Results

Muscle weight and girth were statistically higher in the induced membrane subgroup compared to control rats. The average muscle weight in the induced membrane group was 46.25% vs. control group (33.19% ;p = 0.009). The average muscle girth in the induced membrane group was 78.25% vs. control (60.73% ; p = 0.012). No significant difference was seen between groups in axon counts and muscle force. At 12 weeks post-reconstruction, the induced membrane group had significantly higher SFI scores compared to controls (p = 0.023).

Conclusion

By inseting PNA within an induced pseudomembrane sheath, we were able to significantly enhance muscle reinnervation as demonstrated by increased muscle mass and girth as well as enhancement of motor recruitment demonstrated by SFI. These are promising results for enhancement of allograft nerve reconstruction necessitating further investigation.

9. Osteocyte-specific endocannabinoid receptor 1 (CB1) deficiency influences cancellous bone mass, but does not affect bone response to disuse.

Rachel C. DeNapoli, Evan G. Buettmann, Jolene J. Windle, Aron H. Lichtman, Henry J. Donahue

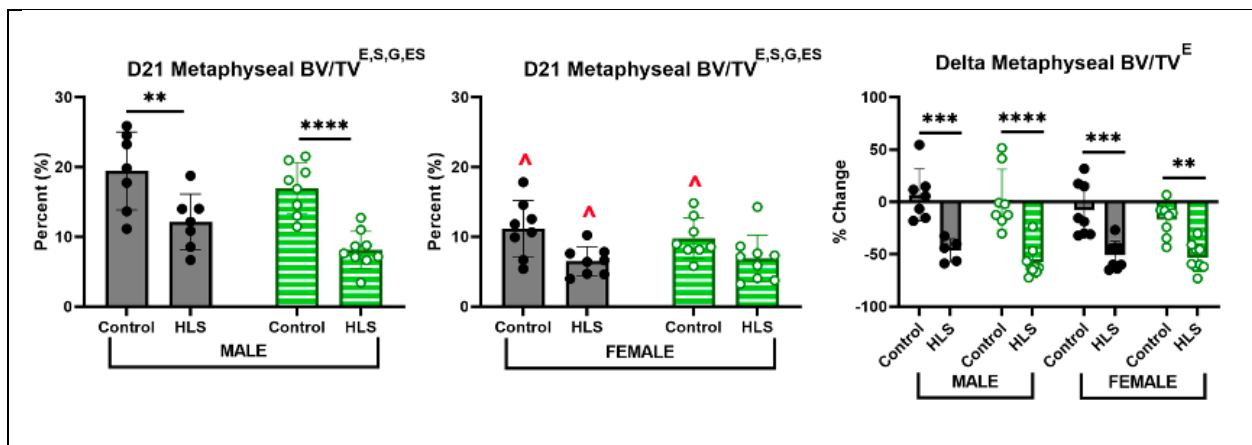
Disuse-induced bone loss is a major health and financial concern for the general population. Endocannabinoid receptor 1 (CB1) influences bone in an age, sex, and strain dependent manner. In particular, our lab found skeletally mature male C57BL/6J mice with a global CB1 deletion (KO) are more sensitive to disuse-induced bone loss than male wildtype, while disuse-induced bone loss was mitigated in female KO mice during single limb immobilization¹. To further determine CB1's role in bone, we hypothesized that mice with a conditional knockout of CB1 in osteocytes, the predominate mechanoregulatory cell in bone, would be more sensitive to bone loss than wildtype during hindlimb suspension (HLS).

We generated novel homozygous DMP1-Cre(+); CB1^{flx/flx} mice (cKO) and DMP1-Cre(-); CB1^{flx/flx} mice (WT) for this experiment. 20-week-old male and female mice (n=7-9/group) were assigned to either HLS or control group for 21 days. Skeletal phenotype was assessed using *in vivo* micro-CT scans. Cancellous bone at epiphyseal and metaphyseal regions were analyzed. Data were analyzed using 3-way ANOVA with Sidak post-hoc test (p<0.05).

MicroCT analysis at D21 demonstrated that loss of CB1 in DMP1 expressing cells led to lower metaphyseal and epiphyseal BV/TV versus WT. HLS resulted in all groups experiencing bone loss from baseline in the metaphyseal and epiphyseal region. However, genotype had no influence on disuse-induced bone loss. In the epiphyseal region, there was an interaction of HLS and sex, with male mice having greater disuse-induced decreases in BV/TV from baseline than female mice.

These results suggest for the first time that CB1 expression in DMP1 lineage cells plays an important role in cancellous bone mass regulation, but not in the response to disuse. These results, when compared to our previous studies, suggest CB1 receptor in osteocytes controls bone mass under basal conditions, while deficiency in earlier osteoblastic cells may control response to disuse.

[1] DeNapoli, R. C. et al. *Journal of Biomechanics* (2023)



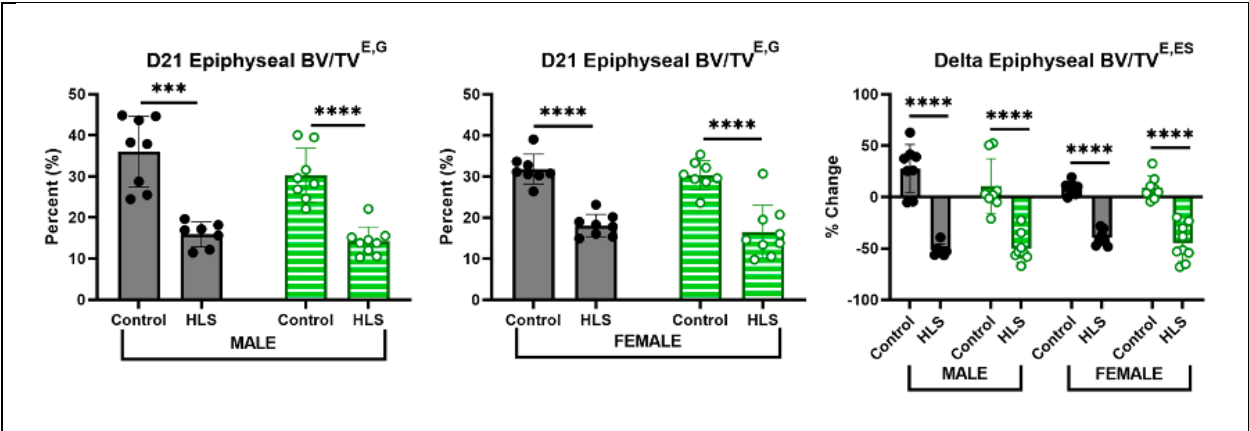


Figure 1: Femoral metaphyseal and epiphyseal trabecular bone BV/TV for male and female WT (filled, black) and cKO (striped, green) at day 21 of HLS and change from baseline. Data depict mean \pm standard deviation. Significant main effects on HLS (E), Sex (S), Genotype (G), and interaction between HLS and Sex (ES). $^{\wedge}p < 0.05$ vs same limb of opposite sex, * $p < 0.05$, ** $p < 0.01$, *** $p < 0.001$, **** $p < 0.0001$

10. Effect of Cyclic Stretch in Engineered Ligaments Depends on Degree of Hierarchical Collagen Organization

Leia Troop¹ and Jennifer L. Puetzer¹

¹Department of Biomedical Engineering, Virginia Commonwealth University, Richmond, VA

Objective: Hierarchical collagen fibers are the primary source of strength in tendons and ligaments, however these fibers do not regenerate after injury or with repair, resulting in limited treatment options. We previously developed a culture system that guides ACL fibroblasts to produce native-sized fibers and fascicles by 6 weeks. These constructs are promising ligament replacements, but further maturation is needed. Mechanical cues are critical for development *in vivo* and in engineered tissues; however, the effect on larger fiber and fascicle formation is largely unknown. The objective here was to investigate whether intermittent cyclic stretch, mimicking rapid muscle activity, drives further maturation in our system to create stronger engineered replacements and to explore whether cyclic loading has differential effects on cells at different degrees of collagen organization to better inform rehabilitation protocols.

Methods: To form constructs, bovine ACL fibroblasts were mixed with collagen and cast into sheet gels at 20mg/mL collagen and 5×10^6 cells/mL. Rectangles were cut from gels, divided between groups, and cultured for up to 6 weeks. Groups included static culture, and 5% or 10% cyclic strain at 1 Hz for 1 hr, twice daily, 3x a week to evaluate dose effect of cyclic loading. Post culture, hierarchical collagen organization, matrix composition, and tissue tensile properties were evaluated.

Results: Cyclic loading drove cells to increase hierarchical collagen organization, collagen crimping, and tissue mechanics. Further, the effect of loading on cells varied depending on the degree of organization. Specifically, 10% load drove early improvements in mechanics and composition, while 5% load was more beneficial later in culture, suggesting a cellular response threshold.

Conclusion: This study provides new insight into how cyclic loading affects cell-driven hierarchical fiber formation and maturation. A better understanding of how mechanical cues regulate fiber formation will help to develop better rehabilitation protocols and better engineer replacements.

11. T cells Contribute to Macrophage Polarization and MSC Recruitment During Osseointegration

Derek Avery, Lais Morandini, Melissa Gabrie, Luke Sheakley, Matthieu Peralta, Henry J. Donahue¹, Rebecca K. Martin², Rene Olivares-Navarrete

¹Department of Biomedical Engineering, Virginia Commonwealth University, Richmond, VA, ²Department of Microbiology and Immunology, School of Medicine, Virginia Commonwealth University, Richmond, VA

Objective: T cells are adaptive immune cells found in lymph nodes, spleen, and bone marrow that significantly affect inflammation and wound healing. CD4⁺ and CD8⁺ T cells, subsets of the $\alpha\beta$ T cell family, are essential for inflammatory cytokine production and immunomodulation of inflammatory innate immune cells. While the role of innate immune cells in response to biomaterials has been explored, the function of T cells in the inflammatory response after implantation is unclear. This study aimed to elucidate immune cell crosstalk and the innate immune response to modified titanium (Ti) implants in the presence and absence of T cells.

Methodology: For *in vivo* studies, smooth, rough, or rough hydrophilic Ti rods were implanted in the femoral canals of 12-week-old male C57BL/6J (*Tcra*^{+/+}) or mice null for $\alpha\beta$ T cells (*Tcra*^{-/-}) (n=6 mice/variable). Mice were euthanized after 3, 7, or 14 days, and peri-implant bone marrow was collected for immunophenotyping analysis by flow cytometry. We characterized neutrophils, pro- and anti-inflammatory macrophages, dendritic cells, and mesenchymal stem cells (MSCs). Data were analyzed by ANOVA with Tukey HSD assessment of differences.

Results: Mice lacking $\alpha\beta$ T cells had significantly higher neutrophils and pro-inflammatory macrophages, fewer dendritic cells and anti-inflammatory macrophages, and reduced recruitment of MSCs from day 3 to day 14 post-implantation on all surfaces. Innate immune cell response to surface modifications was abrogated in the absence of $\alpha\beta$ T cells. Bone formation around Ti implants was significantly reduced in mice lacking $\alpha\beta$ T cells.

Conclusion: Together our results demonstrate that T cells are critical during the inflammatory response and resolution to modified Ti implants, attenuating inflammatory innate immune cells and enhancing MSC recruitment and proliferation. Absence of $\alpha\beta$ T cells compromises bone formation around implants.

12. Non-alcoholic fatty liver disease is associated with skeletal fragility in DIAMOND mice

Authors: Galen M Goldscheitter, Alexandra M Hooks, Mulugeta Seneshaw, Evan G Buettmann, Arun J Sanyal, Henry J Donahue

Introduction: Non-alcoholic fatty liver disease (NAFLD) affects ~1 in 4 people globally and is associated with decreased bone mineral density and increased risk of fracture.^{1,2,3} However, the complete mechanisms connecting NAFLD and bone metabolism are unclassified. This is, largely, due to the absence of an adequate preclinical model. The DIAMOND mouse, uniquely, develops NAFLD under a prolonged high-fat “Western” diet, like humans. Their disease course mimics the human phenotype without noxious agents, allowing us to study both hepatic and extrahepatic effects of NAFLD.⁴ Here, we demonstrate that DIAMOND mice develop bone disease alongside NAFLD.

Methods: DIAMOND mice were fed a Western Diet (Harlan TD.88137) plus sugar water (23.1 g/L d-fructose +18.9 g/L d-glucose) (WD/SW) or a chow diet plus normal water (CD/NW) for 16 or 48 weeks. The femurs and tibias were excised and μ CT scanned (Bruker SkyScan 1276) and then broken in 3-point bending with the posterior (femur) and anterior-medial (tibia) side in tension (Bose ElectroForce 3200).

Results: Marked decreases in bone volume fraction occurred in both the femur and tibia, with significant cortical thinning in the tibia. The ultimate stress borne by tibias and femurs from WD/SW DIAMOND mice after 48 weeks was significantly lower than CD/NW. At 16 weeks, cortical expansion has occurred, but is insufficient to reduce the bone volume fraction or mechanical properties. (Tibial data shown in Figure 1)

Discussion/Conclusions: We observed time- and NAFLD-dependent decreases in skeletal strength at 48 weeks. These decreases are correlated with deleterious changes in bone geometry on μ CT, like those seen in people with NAFLD.⁵ At 16 weeks, early geometry changes are observed without bulk architecture or mechanical strength changes, suggesting the need for longer diet exposure. These results suggest DIAMOND mice are an excellent model to examine the mechanisms underlying bone loss in NAFLD.

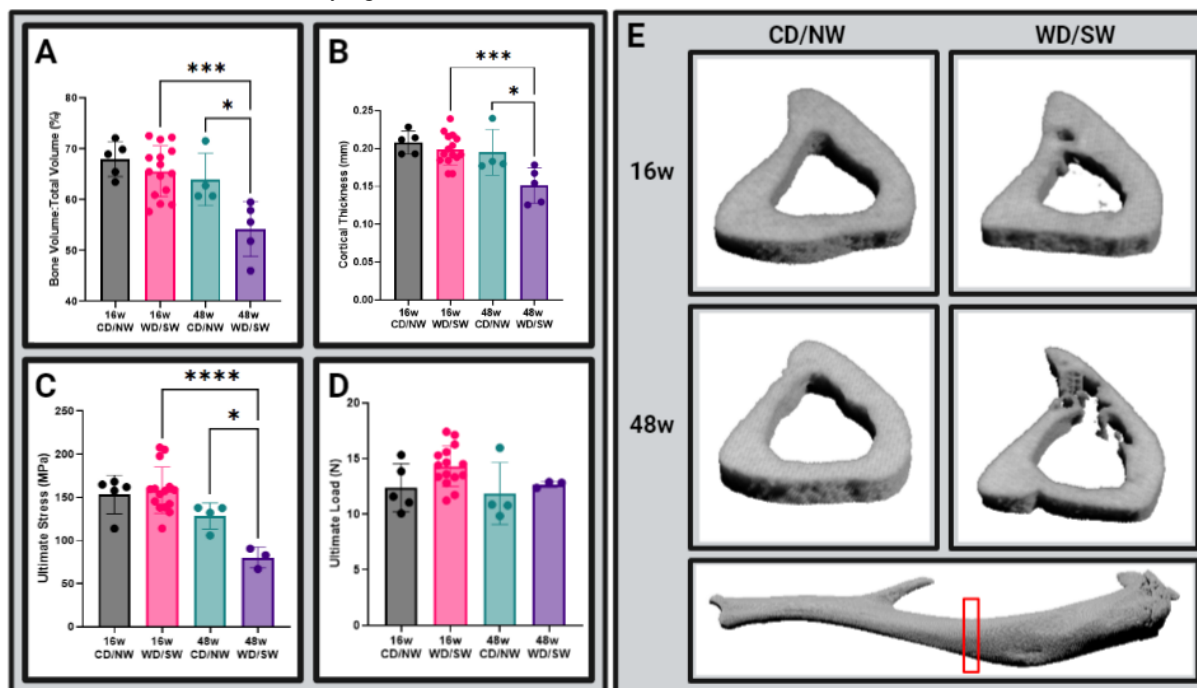


Figure 1. A Tibial bone volume fraction at the mid-diaphysis. B Tibial cortical thickness at the mid diaphysis. C Ultimate stress before failure in 3-point bending. D Ultimate load before failure in 3-point bending. E Representative tibia sections at the mid diaphysis. * $p < 0.05$, ** $p < 0.01$, *** $p < 0.001$, **** $p < 0.0001$. 16w CD/NW (N=5), 16w WD/SW (N=15), 48w CD/NW (N=4), 48w WD/SW (N=5). For ultimate stress and load: tibiae from two 48w WD/SW mice were broken within the span of the supports and could not be evaluated.

References:

1. Younossi ZM, Koenig AB, Abdelatif D, Fazel Y, Henry L, Wymer M. Global epidemiology of nonalcoholic fatty liver disease-Meta-analytic assessment of prevalence, incidence, and outcomes. *Hepatology*. 2016 Jul;64(1):73-84. doi: 10.1002/hep.28431. Epub 2016 Feb 22. PMID: 26707365.

2. Su YH, Chien KL, Yang SH, Chia WT, Chen JH, Chen YC. Nonalcoholic Fatty Liver Disease Is Associated With Decreased Bone Mineral Density in Adults: A Systematic Review and Meta-Analysis [published online ahead of print, 2023 May 30]. *J Bone Miner Res.* 2023;10.1002/jbmr.4862. doi:10.1002/jbmr.4862
3. Pan B, Cai J, Zhao P, Liu J, Fu S, Jing G, Niu Q, Li Q. Relationship between prevalence and risk of osteoporosis or osteoporotic fracture with non-alcoholic fatty liver disease: A systematic review and meta-analysis. *Osteoporos Int.* 2022 Nov;33(11):2275-2286. Doi: 10.1007/s00198-022-06459-y. Epub 2022 Jun 28. PMID: 35764892.
4. Asgharpour A, Cazanave SC, Pacana T, Seneshaw M, Vincent R, Banini BA, Kumar DP, Daita K, Min HK, Mirshahi F, Bedossa P, Sun X, Hoshida Y, Koduru SV, Contaifer D Jr, Warncke UO, Wijesinghe DS, Sanyal AJ. A diet-induced animal model of non-alcoholic fatty liver disease and hepatocellular cancer. *J Hepatol.* 2016 Sep;65(3):579-88. Doi: 10.1016/j.jhep.2016.05.005. Epub 2016 May 31. PMID: 27261415; PMCID: PMC5012902.
5. Barchetta I, Lubrano C, Cimini FA, Dule S, Passarella G, Dellanno A, Di Biasio A, Leonetti F, Silecchia G, Lenzi A, Cavallo MG. Liver fibrosis is associated with impaired bone mineralization and microstructure in obese individuals with non-alcoholic fatty liver disease. *Hepatol Int.* 2023 Apr;17(2):357-366. doi: 10.1007/s12072-022-10461-1. Epub 2022 Dec 15. PMID: 36520377.

13. Estrogen induced osteolysis in triple negative breast cancer mediated by estrogen receptor alpha 36

David J Cohen¹, Cydney Dennis*¹, Jingyao Deng¹, Zvi Schwartz^{1,2}, Barbara D Boyan^{1,3}

¹Department of Biomedical Engineering, Virginia Commonwealth University, Richmond, VA 23284, USA.

²Department of Periodontics, The University of Texas Health Science Center at San Antonio, San Antonio, TX 78229 USA.

³Wallace H. Coulter Department of Biomedical Engineering, Georgia Institute of Technology, Atlanta, GA 30332, USA.

*Presenting Author

INTRODUCTION: Triple negative breast cancer (TNBC) is an aggressive form of cancer characterized by a lack of estrogen receptor alpha 66 (ERa66), progesterone receptor, and HER2. There are 3 known isoforms of ERa that bind to estrogen to regulate breast cancer metastasis: ERa66, ERa46, and ERa36. Due to the lack of ERa66, the most recognized receptor, TNBC is questioned as hormone responsive cancer. Many ERa66 negative breast cancers positively express ERa36. ERa36 is associated with the plasma membrane and binds to 17 β -estradiol (E2) to regulate physiological responses like metastasis through a rapid membrane pathway. Over 70% of metastatic breast cancer metastasizes to the bone and survival rate decreases. Tamoxifen is a common hormonal therapy that reduces tumor progression by binding to ERa66 to block E2 from activating its signaling pathways. It is unclear if tamoxifen can also block the ERa36 receptor pathways. **PURPOSE:** This study evaluated the effect of E2 on TNBC; investigated the mechanism involved; and examined the therapeutic potential of tamoxifen on TNBC. **METHODS:** Ovariectomized mice were used to deplete estrogen in the body, eliminating the variability of already established systemic E2. Mice were implanted with the TNBC cell line, MDA-MB-231 into the bone marrow and separated into 3 groups: sham, ovariectomy, and ovariectomy treated with E2. 8 weeks after implantation and treatment, legs were harvested for microCT. Next, to assess the role of membrane associated E2 receptor-mediated mechanisms of E2 action, MDA-MB-231 cells were treated with E2-BSA for 9 minutes with or without an antibody against ERa36. Conditioned media were collected and used to treat human osteoclast precursors for 7 days then assessed for osteoclast activation. In another experiment, RAW264.7 osteoclasts were treated with conditioned media from E2-BSA treated MDA-MB-231 cells then evaluated for mRNA of osteoclast activation markers CTSK, CLCN7, TRAP, and NFATc1. The final aim separated mice into 4 groups: control, tamoxifen, E2, and an E2/tamoxifen combination group. MDA-MB-231 cells were implanted and mice were given their respective treatment. **RESULTS:** E2 increased the occurrence of osteolysis and fracture but the bone volume remaining was reduced compared to both contralateral and sham legs. E2-BSA increased osteoclast activation, but this effect was lost when treated with anti-ERa36 antibody. E2-BSA treatment increased CLCN7, CTSK, and TRAP, but had no effect on NFATc1. Tamoxifen and E2 separately increased the occurrence of osteolysis and fracture but had no effect on tumor volume compared to control. The combination increased tumor volume and reduced remaining bone volume. **CONCLUSIONS:** These data suggest that estrogen increased osteolysis in TNBC through a membrane mediated pathway involving ERa36 and tamoxifen is unable to block this effect. This pathway could play a role in tamoxifen resistance.

14. The Effect of Genetic Variability on Muscle Mass and Strength from Disuse

Jessica R. Cornthwaite, Michael A. Friedman, Henry J. Donahue

OBJECTIVE: Disuse, in the form of mechanical unloading, is known to decrease muscle mass as well as decrease muscle strength. Our lab has previously shown that simulated disuse causes a loss of muscle mass and strength in genetically diverse inbred mice, however, the effect of genetic variability on muscle loss has not yet been studied. The objective of this project is to determine the effects of genetic variability of muscle loss due to disuse in a diversity outbred (DO) mouse population, which were created by cross-breeding 8 well-characterized founder strains. Therefore, in this project we hypothesize that genetic variability will affect the magnitude of skeletal muscle mass and strength from disuse in the form of single limb immobilization (SLI).

METHODOLOGY: Ten male and ten female 16-week-old DO mice were right limb immobilized by a cast for 21 days, then sacrificed for analysis. Gastrocnemius muscles were micro-CT scanned at baseline as well as lower limbs tested for muscle strength. These same properties were again measured *in vivo* immediately before sacrifice.

RESULTS: Male mice had significantly increased mean cross-sectional muscle area and muscle volume from baseline compared to the females, who showed no effect in muscle mass due to disuse. (Fig. 1) Given that male mice have greater muscle mass at baseline, these data are suggestive of increased inflammation and swelling in the casted leg of male mice. In addition, after three weeks of casting gastrocnemius tetanus force was lower in the immobilized limb of male, but not in the females. (Fig. 2)

CONCLUSION: Previous studies have not investigated the influence of genetic variability on skeletal muscle due to disuse. Based on these current data, we can conclude that genetic variability as well as sex significantly influences skeletal muscle response to disuse. Future investigations of this data include RNA-sequencing of gastrocnemius tissue to determine specific genetic phenotypes present that influence skeletal muscle response to disuse.

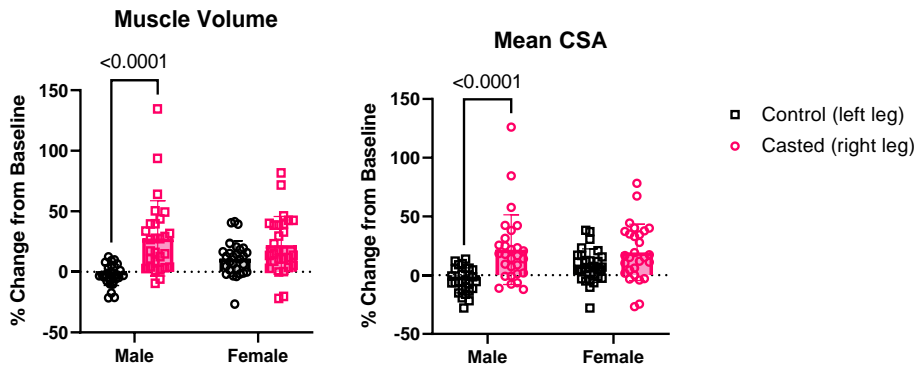


Figure 1. Gastrocnemius muscle volume and mean cross-sectional area in male and female after three weeks of single limb immobilization of the right leg. (Statistical analysis: 2-way ANOVA)

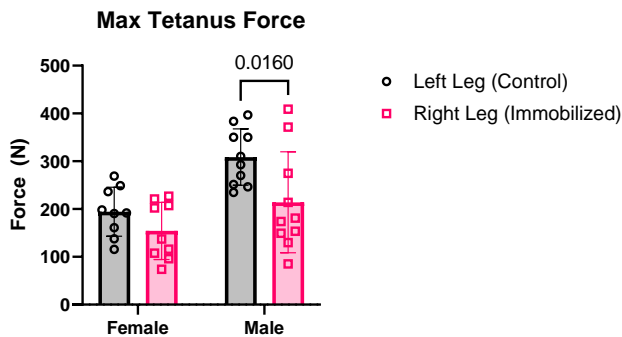


Figure 2. Gastrocnemius lower limb forces after three weeks of single limb immobilization of the right leg. (Statistical analysis: 2-way ANOVA)

15. Investigating the Role of Focal Adhesion Kinase in Hierarchical Collagen Fiber Formation for Musculoskeletal Repair

Tristan Strayer,¹ Leia Troop,¹ and Jennifer L. Puetzer¹

¹Department of Biomedical Engineering, Virginia Commonwealth University, Richmond, VA

Objective: Collagen fibers are the primary source of strength in tendons and ligaments. Cells organize these fibers hierarchically, assembling them from nm-wide fibrils to larger fibers and fascicles with increasing mechanical demands. These fibers do not regenerate after injury, nor in engineered replacements. A better understanding of the mechanotransduction pathways that regulate cell-driven collagen organization is critical to developing functional repairs. One way cells sense environmental-cues is through focal adhesions regulated via focal adhesion kinase (FAK). Focal adhesions are reported to play a major role in fibril formation, but their role at larger-scales of organization is unknown. Previously, we developed a culture device that guides ACL fibroblasts to develop aligned fibrils by 2 weeks, and larger fibers and fascicles by 4 and 6 weeks, respectively. Using this system, our objective is to evaluate how cues translated via focal adhesions regulate cellular development of hierarchical fibrils, fibers, and fascicles.

Methods: To form constructs, ACL fibroblasts were seeded into 20mg/ml collagen at 5×10^6 cells/mL and cultured in our device for up to 6 weeks to guide hierarchical fiber development. To investigate the role of FAK during fibril, fiber, and fascicle formation, constructs were dosed with 10uM FAK inhibitor PF-228 from 0-2 weeks, 2-4 week, or 4-6 weeks, respectively. Control constructs were treated with DMSO as a vehicle control or cultured in standard DMEM. Post culture, collagen organization, matrix composition, and tissue tensile properties were evaluated.

Results: As expected, FAK inhibition during fibril formation significantly reduced collagen organization and tensile properties compared to controls. However, FAK inhibition during fiber and fascicle formation had little-to-no effect on degree of organization or mechanics.

Conclusions: Collectively, this suggests cell-ECM connection via FAK-cytoskeletal signaling is key to early stages of hierarchical formation, but plays a smaller role in later stages. Ongoing work is evaluating additional mechanotransduction pathways.

16. Axial Compression of Tibia Increases Marrow Macrophage and T-Cell Subsets in a Load-Dependent Manner

Evan G. Buettmann¹, Lais Morandini¹, Joseph A. Denisco¹, Jerin Jose¹, Galen Goldscheitter¹, Michael A. Friedman¹, Henry J. Donahue¹, Rene Olivares-Navarrete¹

¹Department of Biomedical Engineering, Virginia Commonwealth University, Richmond, VA

Introduction: The immune system dysregulation is linked to negative changes in bone mass and osteoporosis.¹ Axial bone loading is a known anabolic treatment to increase bone mass via WNT- β -catenin upregulation.^{2,3} Although, WNT- β -catenin upregulation is known to altering immune cell populations within the bone marrow⁴, the role of tibial loading in inducing these same alterations is unknown.

Methods: Male 16-week C57BL/6J mice underwent *in vivo* tibial loading (right limb only) under anesthesia for three consecutive days (60 cycles, 2Hz triangle waveform) from 0.5N to 4N or 9N similar to waveforms used previously.^{5,6} Mice undergoing anesthesia and preload (-0.5N) but no dynamic loading served as sham controls. All mice received buprenorphine ER lab (0.5mg/kg, s.c.) throughout loading. Mice were euthanized one day after cessation of loading and tibial cortical bone underwent qPCR while marrow underwent flow cytometry analysis. Data analysis used 2-WAY Repeated measures ANOVA for effect of load (right versus left limb) and load level (sham, 4N, 9N).

Results: 9N loaded limbs showed significantly increased *Coll1a1* expression relative to nonloaded control limbs (**Figure 1A**). In addition, 9N loaded group showed decreased SOST expression in both tibiae compared to over load levels demonstrating increased anabolism. Macrophages (F4/80⁺/CD11c⁻ of CD45⁺) and T-Cells (CD3⁺ of CD45⁺) showed significant dose-dependent increases in marrow populations based on load magnitude and limb (p<0.05; **Figure 1B**). Mast cells were elevated in loaded limbs overall they showed no significant changes due to load level and B-cells were unaffected by any parameters (p >0.05).

Discussion: Our results suggest that tibial loading induces significant upregulation of macrophages and T-cells in bone marrow in a dose-dependent manner. Previous results from our group have shown that these same cell immune cell populations are most differentially responsive to orthopedic implant substrate.⁴ These results suggest that macrophages and T-cells are highly mechanoresponsive and future research is needed to determine their dispensability in the anabolic responses to bone loading.

Acknowledgements: This work is supported by the Translational Research Institute through NASA Cooperative Agreement NNX16AO69A

References:

1. Tsukasaki, M. and H. Takayanagi, *Osteoimmunology: evolving concepts in bone-immune interactions in health and disease*. Nature Reviews Immunology, 2019. **19**(10): p. 626-642.
2. Chermiside-Scabbo, C.J., et al., *Old Mice Have Less Transcriptional Activation But Similar Periosteal Cell Proliferation Compared to Young-Adult Mice in Response to in vivo Mechanical Loading*. J Bone Miner Res, 2020. **35**(9): p. 1751-1764.
3. Lawson, L.Y., et al., *Osteoblast-Specific Wnt Secretion Is Required for Skeletal Homeostasis and Loading-Induced Bone Formation in Adult Mice*. J Bone Miner Res, 2022. **37**(1): p. 108-120.
4. Avery, D., et al., *Canonical Wnt signaling enhances pro-inflammatory response to titanium by macrophages*. Biomaterials, 2022. **289**: p. 121797.
5. Sun, D., et al., *Evaluation of loading parameters for murine axial tibial loading: Stimulating cortical bone formation while reducing loading duration*. J Orthop Res, 2018. **36**(2): p. 682-691.
6. Main, R.P., et al., *Murine Axial Compression Tibial Loading Model to Study Bone Mechanobiology: Implementing the Model and Reporting Results*. Journal of Orthopaedic Research, 2020. **38**(2): p. 233-252.

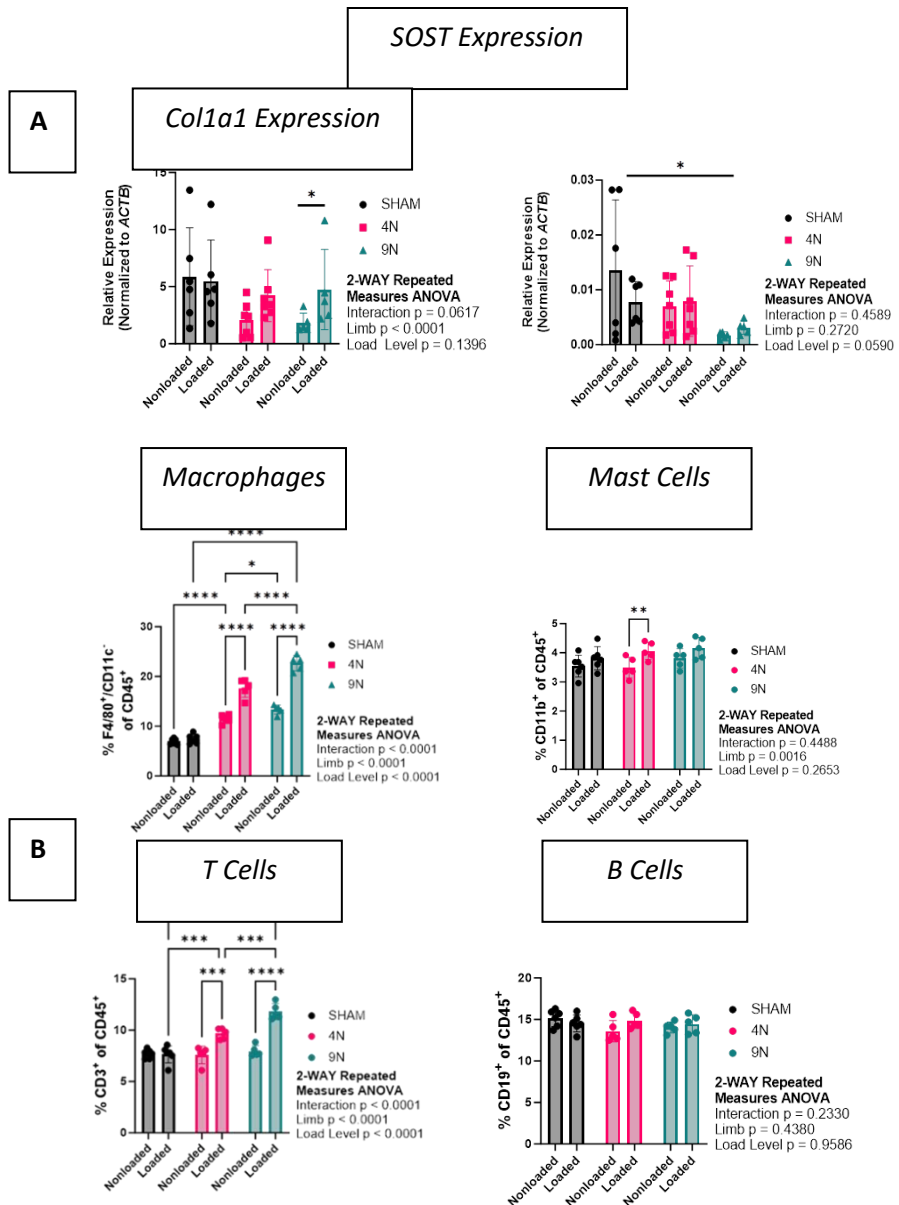


Figure 1. A. Changes in cortical bone gene expression following 3 loading bouts **B:** Changes in bone marrow immune cell populations following 3 loading bouts. * p < 0.05 by Tukey's post-hoc test following 2-WAY Repeated Measures ANOVA: data presented as mean ± SD

17. Unraveling the Role of Advanced Glycation End-Products in Age-Related Human Meniscus Degeneration

Austin G. Gouldin,¹ Nirav K. Patel,² Gregory J. Golladay,² Jennifer L. Puetzer^{1,2*}

¹Departments of Biomedical Engineering and ²Orthopaedic Surgery, Virginia Commonwealth University, Richmond, VA, United States

Objective: In the meniscus there is a clear link between increasing age and degeneration, leading to increased injuries, progressive osteoarthritis, and often total knee replacements. Advanced glycation end-products (AGEs) are non-enzymatic crosslinks that accumulate in collagen with age, altering tissue mechanics and cell function, leading to increased injury and inflammation. Due to the high reliance on collagen in the meniscus, AGEs are believed to play a central-role in age-related degradation and have been shown to significantly increase with age. However, little is known regarding regional accumulation of AGEs, and AGEs impact on collagen structure, tissue mechanics, and cell function in menisci. The objective of this study was to characterize changes in aged osteoarthritic (OA) menisci, specifically evaluating zonal AGE accumulation, to gain a better understanding of changes that may lead to age-related meniscal degeneration.

Methodology: 48 deidentified human menisci (52-84 years of age) were obtained from subjects that underwent total knee replacements. Specific changes in the extracellular matrix (ECM) were assessed through biochemical assays, gross morphology, and confocal analysis. Deoxyribonucleic acid (DNA), Glycosaminoglycan (GAG), collagen, and AGE accumulation were compared with patient age, zonal region, and patient sex.

Results: There were minimal changes in DNA, GAG, and collagen concentration with age or zone. However, collagen fraying and AGEs increased with age, with more AGEs accumulating in the meniscal horns compared to the central body, and in male menisci compared to females.

Conclusions: These findings provide greater insights into the regional changes that occur in human menisci with age and OA. Specifically, these results suggest AGEs play a role in meniscus degeneration, and may be a potential therapeutic target to reduce age-related tears, degeneration, and OA progression. Ongoing work is evaluating the potential of aged OA meniscal cells to regenerate collagen fibers with and without AGEs to better drive regeneration with age.

18. Genetic Variation Affects the Magnitude of Bone and Muscle Loss from Disuse

Michael A. Friedman¹, Jessica Cornthwaite¹, John McKean¹, Zhane Davis¹, Gabriel A. Hoppock¹, Yue Zhang¹, Evan G. Buettmann¹, Steven Meas¹, Gabriella M. Daire¹, Charles R. Farber², Henry J. Donahue¹

¹Virginia Commonwealth University, Richmond, VA; ²University of Virginia, Charlottesville, VA

Disuse occurs after all musculoskeletal injuries, surgeries, and spaceflight. Disuse decreases bone and muscle mass, increasing the risk of future injury. Genetic variation affects bone and muscle mass, but it remains unclear how genetics affects the response to disuse. To investigate the effects of genetic variation on disuse, we used genetically diverse, outbred mice. We hypothesized that genetic variation affects the magnitude of bone and muscle loss from disuse via immobilization. 28 female and 29 male adult outbred mice (J:DO strain) had the right hindlimb immobilized for 3 weeks. Then, bone and muscle mass and strength of each limb were evaluated.

Immobilization decreased femur bone volume and cortical area (Figure 1). Femur strength was lower in the immobilized limb in female mice. Gastrocnemius mass was lower in the immobilized limb (Figure 2). Genetic variation was the highest source of variation in bone and muscle properties, accounting for 32-99% of variation in each property measured.

This was the first study to examine the effects of any intervention on bone and muscle in a genetically diverse mouse population. We found genetic variation heavily influences the magnitude of response to disuse. These results suggest the response to disuse is heritable, meaning the magnitude of response is influenced by genetic factors. All mice experienced bone and muscle loss from immobilization, suggesting there are common underlying mechanisms of bone and muscle loss that exist regardless of genetics. Genetic variation, limb and sex influence bone and muscle mass, underscoring the importance of evaluating interventions in both sexes, both limbs and a genetically diverse population. Using this animal model, we have identified mechanisms to target for therapeutic interventions that will apply to a genetically diverse patient population.

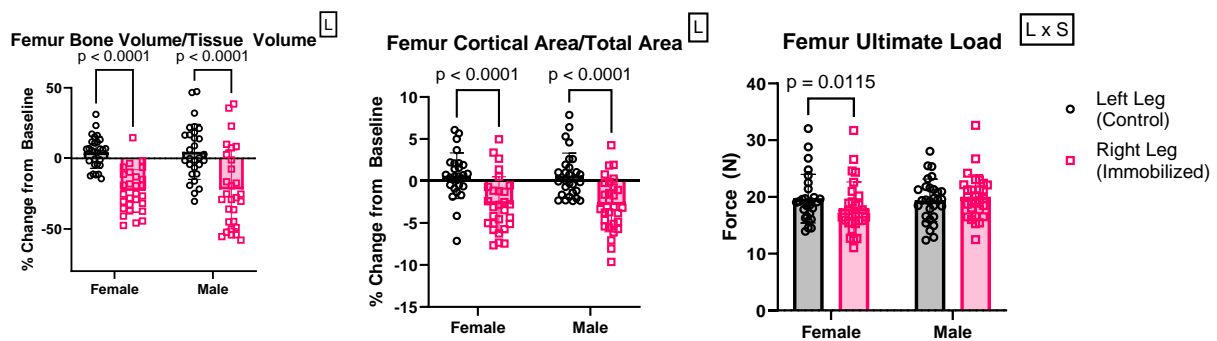


Figure 1. Femur epiphyseal BV/TV, mid-diaphyseal cortical area fraction, and ultimate load (mean \pm SD) after three weeks of single limb immobilization of the right leg in 16-week old diversity outbred mice. Immobilization decreased bone mass in male and female mice and decreased bone strength in female mice. L - significant main effect of limb; L x S - significant limb x sex interaction (2-Way RM ANOVA).

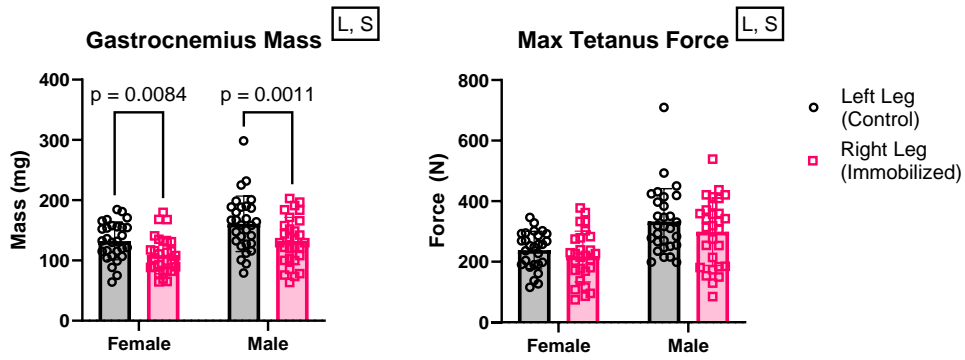


Figure 2. Gastrocnemius mass and lower leg muscle force (mean \pm SD) after three weeks of single limb immobilization of the right leg in 16-week old diversity outbred mice. Immobilization decreased muscle mass in all mice. L - significant main effect of limb; S - significant main effect of sex (2-Way RM ANOVA).

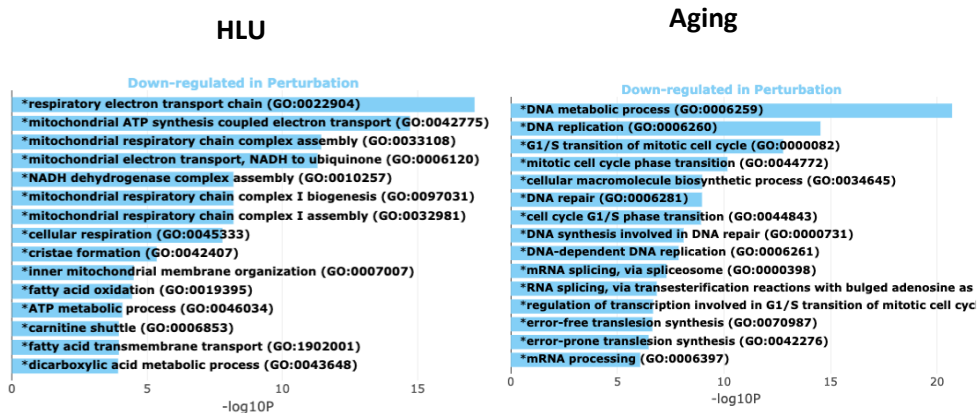
19. Hindlimb Unloading Induces Microarchitectural and Transcriptomic Changes in the Femur and Tibia in an Age- and Sex-Dependent Manner

Steven J. Meas, Michael A. Friedman, Gabriella M. Daire, Henry J Donahue

Age and disuse-related bone loss both result in decreases in BMD, cortical thickness, and trabecular thickness and connectivity. Thereby, it is an emerging concept that disuse induces physiological changes in bone like those seen with aging. This study is the first to examine the role of senescence in disuse-related bone loss, to directly compare the phenotype in age- and disuse-related bone loss. Animal studies used 4-month, 6-month, and 22-month C57BL/6J male and female mice that were hind-limb unloaded (HLU) for 3 weeks. Ingenuity Pathway Analysis included a publicly available dataset (GLDS647) from 3-month female C57BL/6 mice unloaded for 7 days.

In females, three weeks of HLU induced an intermediary bone phenotype in femurs between 6-month-old and 22-month-old mice. Specifically, CTAr/TAr significantly decreased in young HLU mice (n=7) and further in aged control mice (n=13) compared to young ground control mice (n = 7; young control: 55%, young HLU: 48.86%, aged control: 43.25%; $p < 0.0001$). In males, CTAr/TAr remained similar between young control mice (n=8, 42.63%) and young HLU mice (n=8, 42.25%) but there was a decrease in CTAr/TAr with aged control (n=11, 38.91%) and aged HLU mice (n=3, 34.00%). Metaphyseal trabecular bone indices were unchanged. Epiphyseal trabecular bone volume (BV/TV) in female mice was lower in young HLU mice (22.0%) compared to young control (29.7%, $p < 0.05$) and aged control (28.7%, $p < 0.05$) mice. Male mice demonstrated similar trends, with a decrease in BV/TV due to HLU ($p < 0.05$).

Whole-bone marrow-flushed tibias were sequenced and analyzed. Gene ontology analysis demonstrated that mitochondrial function was downregulated after HLU whereas cell-cycle transition was downregulated with aging. These ontologies suggest that HLU leads to dysfunctional mitochondria that can perhaps lead to cellular errors in transcription and translation, whereas in aging there is primarily a downregulation of cell cycle processes. Ingenuity pathway analysis was used to identify the leading canonical pathways and upstream regulators in each HLU age group. IPA identified “Senescence Pathway” as the fourth leading canonical pathway enriched in mice exposed to HLU. HLU induced activation of the senescence pathway in 3 month ($p < 0.05$, $z = 3.464$) and 4 month ($p < 0.001$, $z = 0.6$) old mice, inhibited it in 6 month ($p < 0.01$, $z = -3.153$) old mice and did not change it in 22 month ($p = 0.1$, $z = -1$) old mice.



20. Characterizing Nucleus Pulposus fluid shear stresses and deformation in response to interstitial fluid flow in healthy and degenerate microenvironments

Logan Petry, Joyce Xu, Priscilla Y Hwang

Objective: In vivo, nucleus pulposus (NP) cells are subject to fluid shear stress (FSS) due to tissue hydration and compressive spinal loading, and studies indicate changes in cell morphology and mechanoreponse to shear stress is an initiating factor to disc degeneration pathologies. However, the forces experienced by NP cells, as well as the mechanoreceptors activated in response to shear stress are still largely unknown. Thus, the objective of this study was to understand how different shear stress velocities effect the forces experienced by NP cells and morphology.

Methods: A 2D finite element computational model of an NP cell embedded in Matrigel was developed in COMSOL, and we simulated various fluid flow conditions to mimic static (no flow), healthy (low flow; $v = 1.76 \text{ um/s}$), and degenerate NP (high flow; $v = 0.32 \text{ um/s}$) environments. NP cell stiffnesses were also adjusted for healthy ($E = 0.354 \text{ Pa}$) or degenerate cell ($E = 0.8 \text{ Pa}$) phenotype. We analyzed average normalized von Mises stress, a composite of normal and shear stresses, and average strain over the cell boundary.

Results: We found that NP cells under no flow conditions retain its initial shape since the cell is not subject to FSS. This behavior held true regardless if the cell was healthy or degenerate. Under flow, we found that NP cell average strain increased proportionally to velocity. Investigating cell deformation, our model demonstrated the cell deformed primarily against the direction of flow. Analyzing stresses along the cell membrane, the model demonstrated stress concentrations at the front and rear of the cell, in line with the flow direction and forces on the cell membrane increased with fluid velocity.

Conclusion: Under fluid flow, the forces experienced by NP cells correlates positively with flow speed, regardless of cell stiffness, and form stress concentrations at the cell front and rear. Since the primary direction of cell deformation is against fluid flow, NP cells may develop a geometric polarity and reorient themselves against flow, which we will investigate in future studies.

21. Bolus Fentanyl Induces Prolonged Cardiovascular Dysregulation in SKH-1 Mice

Mackenzie Newman¹, Heather Connery², John Owen¹, Raymond Raylman³, Jonathan Boyd^{1,2}

¹Department of Orthopaedic Surgery, Virginia Commonwealth University, Richmond, Virginia, USA

²Department of Physiology, Pharmacology and Toxicology, West Virginia University, Morgantown, West Virginia, USA

³Department of Radiology, West Virginia University School of Medicine, Morgantown, West Virginia, USA

While fentanyl overdose is common in recreational users, clinical applications of fentanyl can also induce life-threatening conditions such as Wooden Chest Syndrome. Opioid antagonists such as Narcan can reverse some acute symptoms of fentanyl overdose, but they are not entirely effective to combat fentanyl and do not address its long-term impacts. In this study, we investigated the effects of a single, bolus dose of subcutaneous fentanyl on components of the cardiovascular system up to one week post-dose. PET scanning revealed decreased glucose uptake in brain and heart up to 24 hours post-dose, while lungs recovered by 7 days. Fluorescence imaging with indocyanine green, a clinical dye used to detect perfusion and vascular damage, revealed increased heart and lung uptake up to 6 hours post-dose with recovery to baseline by 24 hours. In comparison, brain uptake was significantly decreased compared to controls at 40 minutes post, with recovery thereafter. Multiplex ELISA assay using an immune monitoring 48-plex revealed dysregulated cytokine signaling in hearts and lungs up to 7 days post-dose, in analytes such as betacellulin and eotaxin, while brain cytokines had recovered to baseline. These data show that the symptoms of fentanyl exposure are not limited to acute respiratory depression and are prolonged with the absence of outward symptoms. Future studies are necessary to address the long-term effects of fentanyl on cardiovascular health.

22. RNA Sequencing Analysis of Muscle-Nerve Cross-talk in a Transwell Co-culture Model

James T Redden¹, Zvi Schwartz^{1,2}, Michael J. McClure¹

¹Virginia Commonwealth University, Richmond, VA, ²University of Texas Health Science Center at San Antonio, San Antonio, TX,

Email of Presenting Author: reddent@vcu.edu

Introduction: Motor nerve injuries can contribute to a loss of motor function with a small percentage of injuries regaining adequate strength. The neuromuscular junction (NMJ) plays a key role in dictating functional outcomes, but re-establishing a motor nerve connection with the NMJ is constrained by a regenerative window. The goal of this study was to better understand muscle-nerve signaling in order to identify key targets that are critical for NMJ stabilization.

Methods: C2C12 myoblasts and NSC34 motor neurons were plated in parallel to prepare the cells for eventual co-culture. The experiment generated four groups: C2C12 untreated, NSC34 untreated, C2C12 co-cultured, and NSC34 co-cultured. After 3 days, cells were separately harvested for RNA isolation. Whole RNA sequencing was used and analysis was performed in Rstudio following the DESeq2 Bioconductor pipeline to identify differentially expressed genes. Pathway analysis was performed with the Qiagen Ingenuity Pathway Analysis tools.

Results: Notably, many upregulated genes in the NSC34 cells co-cultured with the C2C12 myotubes were associated with proliferation (Rpl36, Higd1a, Gapdh, Tpi3, Bnip3, Pk3), protein synthesis (Rpl36, Rpl17, Rpl28), and nerve regeneration (Mif). C2C12 cells increased markers associated with increased muscle fiber size (Imp3) which acts via the insulin-like growth factor pathway. Myod1 was upregulated and is a master regulator of muscle fiber formation. Other genes associated with muscle fiber maturation (Mypn) were upregulated suggesting that myotubes had matured faster than no treatment controls. Further research is needed to understand how these signaling pathways are influencing NMJ development and stabilization.

Conclusion: Understanding how muscle-nerve cross-talk influences gene expression in each cell type is crucial for improving clinical outcomes. The described RNA sequencing has been a next step in better understanding each cell type's contribution to NMJ maintenance and an initial exploratory analysis to find potential therapeutic targets to preserve the NMJ following a denervation injury.